Thermal diffusion properties of Zn, Cd, S, and B at the interface of $CuInGaSe_2$ solar cells

Young-Gui Yoon · In-Hwan Choi*

Department of Physics, Chung-Ang University, Seoul 156-756, Korea

ABSTRACT: Two different window-structured $CuInGaSe_2$(CIGS) solar cells, i.e., CIGS/thin-CdS/ZnO:B(sample A) and CIGS/very thin-CdS/Zn(S/O)/ZnO:B(sample B), were prepared, and the diffusivity of Zn, Cd, S, and B atoms, respectively, in the CIGS, ZnO or Zn(S/O) layer was estimated by a theoretical fit to experimental secondary ion mass spectrometer data. Diffusivities of Zn, Cd, S, and B atoms in CIGS were 2.0×10^{-13}(1.5×10^{-13}), 4.6×10^{-13}(4.4×10^{-13}), 1.6×10^{-13}(1.8×10^{-13}), and 1.2×10^{-12} cm^2/s at 423K, respectively, where the values in parentheses were obtained from sample B and the others from sample A. The diffusivity of the B atom in a Zn(S/O) of sample B was 2.1×10^{-14} cm^2/sec. Moreover, the diffusivities of Cd and S atoms diffusing back into ZnO(sample A) or Zn(S/O)(sample A) layers were extremely low at 423K, and the estimated diffusion coefficients were 2.2×10^{-15} cm^2/s for Cd and 3.0×10^{-15} cm^2/s for S.

Key words: CIGS solar cell, Zn(S/O), ZnO:B, thermal diffusion, diffusivity, diffusion coefficient

1. Introduction

A CdS buffer coated by chemical bath deposition(CBD) has shown the highest energy conversion efficiency and is commonly used as a buffer in $CuInGaSe_2$(CIGS)-based solar cells[1]. Nevertheless, some alternative technologies for CdS buffers have been examined[2, 3] due to the absorbance of energy photons at a level greater than its energy band gap, 2.42 eV, and Cd is a harmful heavy metal. The ZnS compound semiconductor has been most widely studied as a substitute for a CdS buffer layer in CIGS solar cells[2]. The principal reasons for using the CBD method in the production of CIGS solar cells are the low processing temperature and the uniform coating. The former can reduce elemental mixing by thermal diffusion at the interface, while the latter increases the shunt resistance of the solar cell. Even though the CBD method has many merits, as mentioned earlier, one drawback to the manufacture of the CIGS solar cell in industry is its wet process.

CIGS solar cells are generally produced with a 50-nm- to 70-nm-thick CdS buffer layer[4] and show some decrease in quantum efficiency(QE) below 500 nm wavelengths because of light absorption by the CdS buffer layer. The light absorption in this region can be minimized if the thickness of the CdS layer can be reduced to minimize the efficiency loss due to this absorption; however, the reverse-bias characteristics in the I-V curve deteriorate under these conditions.

CIGS/t-CdS/ZnO:B(sample A) and CIGS/vt-CdS/ Zn(S/O)/ ZnO:B (sample B) solar cells were prepared in this study. The notation Zn(S/O) indicates the ZnS/ZnO/ZnS/ZnO sequence of the ZnS layer and ZnO layer. The sample A had a single CdS buffer with a thickness of approximately 25 nm, which is the smallest thickness showing comparable stable I-V properties, whereas the thickness of the CdS buffer in sample B was less than 5 nm. Cross-sectional transmission electron microscopy (TEM) images and secondary ion mass spectrometer (SIMS) depth profile of the elements were obtained. SIMS experimental results were analyzed by fitting with a theoretical equation to obtain the diffusivity of each element.

2. Experimental Details

Cu-poor CIGS absorber layers were prepared using a co-evaporation method with a three step process consisting of: (i) the formation of an $(In,Ga)_2Se_3$ layer on Mo-coated soda-lime glass substrates heated to 350℃, followed by (ii) the deposition of Cu and Se at approximately 550℃, and (iii) the addition of more In, Ga and Se at the same substrate temperature.

*Corresponding author: ihchoi@cau.ac.kr
Received February 6, 2013; Revised April 9, 2013; Accepted April 18, 2013

ⓒ 2013 by Korea Photovoltaic Society
This is an Open Access article distributed under the terms of the Creative Commons Attribution Non-Commercial License (http://creativecommons.org/licenses/by-nc/3.0)
which permits unrestricted non-commercial use, distribution, and reproduction in any medium, provided the original work is properly cited.

The x-ray fluorescence-confirmed composition ratios of [Cu]/[III] and [Ga]/[III] of the CIGS absorber layer were approximately 0.93 and 0.37, respectively. The CdS buffer layers were coated onto the CIGS absorber layers by CBD. The chemical solution used for the CdS coating by CBD was prepared by mixing separate solutions of $CdSO_4$ and thiourea in ultra-pure water with a diluted NH_4OH solution in ultra-pure water. CdS thin films were grown on a CIGS absorber layer in the solution heated to 60℃.

Two different CIGS solar cells were prepared:(i) a 25-nm-thick CdS film was coated on the CIGS absorber by CBD, and a boron-doped ZnO window layer was then deposited by MOCVD to produce the CIGS/CdS/ZnO:B structure solar cell, and (ii) < 5-nm-thick CdS film was coated on the CIGS absorber by CBD, and both a Zn(S/O) window layer and a boron-doped ZnO window layer were deposited consecutively by MOCVD to produce the CIGS/Zn(S/O)/ZnO:B structure solar cell.

A first window layer, Zn(S/O), was prepared by the sequential deposition of ZnS/ZnO/ZnS/ZnO layers by MOCVD in the order of flowing precursors of S/Zn/O_2/Zn/S/Zn on heated substrates. Each Zn/S and Zn/O_2 was deposited 30 times, and the deposition times of Zn,S, and O_2 were 4sec each. The purge time between each deposition was 6sec. The boron-doped ZnO window was subsequently deposited on the additional buffer in the same chamber for 10min. The susceptor temperature was kept at 180℃ during deposition of the window layer**.**

The DMZn, t-BuSH, and H_2O precursors were used for Zn, S and O_2, respectively. B_2H_6 gas was used as the boron (B) -doping gas to produce the transparent conducting oxide (TCO) window, ZnO:B. The pressures in all precurs or canisters were 500 torr during deposition, and the flow rate of the carrier gas through the Zn, S, and O_2 precurs or canisters were 30, 60 and 50sccm, respectively. The pressure in the reaction chamber was 0.5torr during deposition.

SIMS was analyzed by a CAMECA IMS 7f magnetic sector SIMS with O_2 primary source. The acceleration voltage and the beam current of the primary source were 10kV and 100nA, respectively. The bias voltage applied to sample was 5kV. To minimize the edge effect the aperture diameter size installed for SIMS analysis was about 33㎛, while the sputtering raster area of the primary beam was 200um x 200um. JEOL JEM-2100F operated at 200kV was used for investigation of cross-sectional TEM image near the junction interface. TEM sample with a thickness of < 50 nm were prepared using a focused ion beam, TESCAN LYRA FEG1.

3. Results and Discussion

Figures 1(a) and (b) show cross-sectional TEM images of CIGS/t-CdS/ZnO:B (sample A) and CIGS/vt-CdS/Zn(S/O)/ZnO:B (sample B) solar cells, respectively. In contrast to the relatively thick CIGS and ZnO or Zn(S/O) layers with large grains, the CdS layer consisted of very thin layers with very small grains. As shown in Fig. 1(b), the CdS buffer layer in sample B was so thin that it could not be distinguished from the window and absorber layer, whereas the CdS layer in Fig. 2(a) shows a

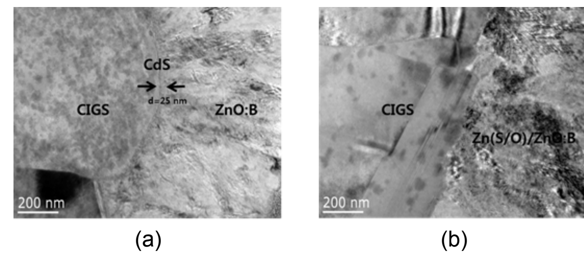

Fig. 1. TEM cross-sectional images of (a) CIGS/CdS/ZnO:B and (b) CIGS/Zn(S/O)/ZnO:B solar cells with a reference scale.

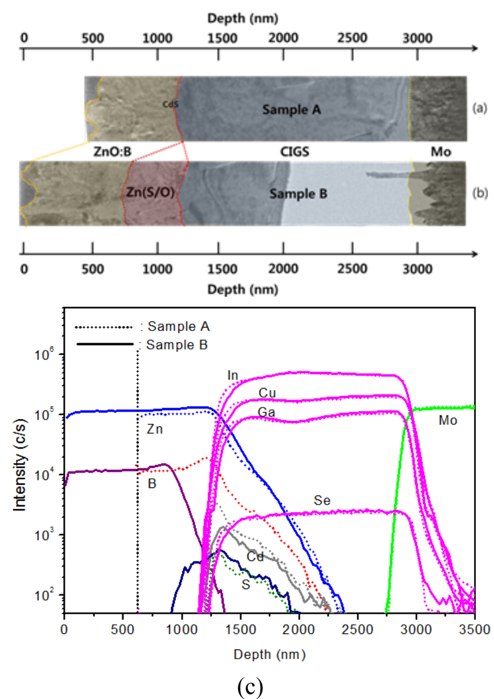

Fig. 2. TEM images of (a) CIGS/CdS/ZnO:B and (b) CIGS/Zn(S/O)/ZnO:B solar cells near the interface of the CIGS absorber layer and buffer layer, and the (c) SIMS depth profile. Note that the coordinate origin is on the top of the ZnO window of sample B.

measurable thickness. Although the CIGS layer exhibited substantial surface roughness, the CdS layer grown on the CIGS had uniform thickness. The estimated and measured thicknesses of the CdS films from the growth rate and TEM results were 25 nm and <5 nm for samples A and B, respectively.

The SIMS depth profile was performed to confirm the diffusion of each element in the CIGS solar cell, and the results are shown in Fig. 2(c). A low magnification TEM image has been included to enhance content understanding in Figs. 2(a) and (b). In Fig. 2(c), the short dots and solid lines indicate the experimental data for samples A and B, respectively. The SIMS signals for Mo, Cu, In, Ga and Se atoms in the rear electrode and absorber layer of samples A and B showed almost the same shapes and intensities and restricted appearance in the region of CIGS absorber layer. On the other hand, the SIMS signals for Zn, Cd and S atoms were not restricted in the region of the buffer but were diffused deeply into the absorber layer.

In the diffusion process, the concentration of impurity atoms at any depth after certain diffusion duration is expressed as

$$N(x,t) = N_0 \operatorname{erfc}\left(\frac{x}{2(Dt)^{1/2}}\right) \quad (1)$$

where erfc indicates the complementary error function that is a transcendental function often encountered in probability and stochastic process theory, is the solid state solubility, and is the diffusion coefficient (diffusivity). In the depth-profiled SIMS data of Fig. 3, the experimental data for Zn, Cd, S and B atoms were theoretically fitted by Eq. (1) to estimate their diffusivity in the CIGS, Zn(S/O) or ZnO layer at 423K. The temperature is the substrate temperature when the ZnO window layer was deposited by MOCVD. The results are shown in Figs. 3(a), (b), (c) and (d), respectively.

Extra care should be taken when performing composition depth profile by using SIMS technique to avoid mixing of the signals from the elements in different depth. There are two major reasons for the mixed signals in SIMS. One is the edge effect, and the other is the recoil effect. The edge effect can be removed by decreasing the aperture size for the detector. The recoil effect can be minimized by reducing the difference between the acceleration voltage of primary beam and the bias voltage applied to sample. The SIMS depth profile data always contain both the mixing effects to some degree. Therefore, the diffusivity study by using SIMS depth profiles is meaningful

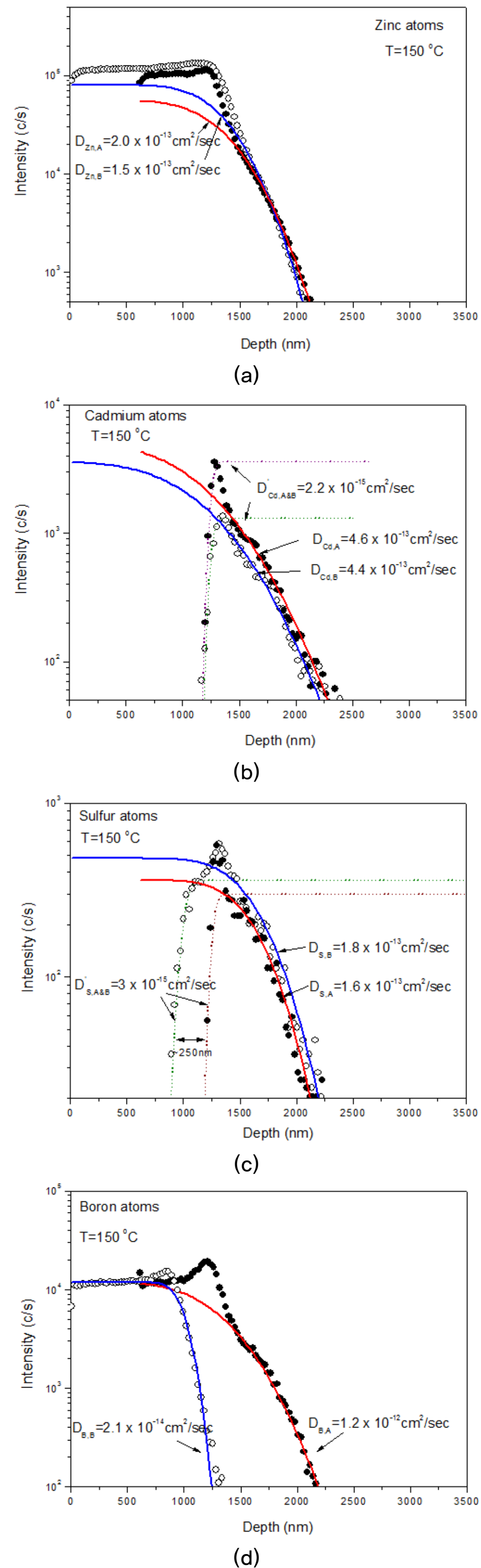

Fig. 3. SIMS depth profile spectra for (a) Zn atoms, (b) Cd atoms, (c) S atoms, and (d) B atoms. The red line is the CIGS/CdS/ZnO:B solar cell, and the blue colored line is the CIGS/Zn(S/O)/ZnO:B solar cell. Brown and green doted lines in(b) and (c) are the CIGS/CdS/ZnO:B and CIGS/Zn(S/O)/ZnO:B solar cells, respectively.

only when the mixing effects are negligible compared to that of the thermal diffusion. To estimate the mixing effects at the experimental conditions, SIMS depth profile data of Zn atom obtained from two different samples were compared. One was the sample used in this study and the other was the sample with ZnS buffer deposited on CIGS absorber by CBD method without any treatment. From this experiment we can be sure that the mixing effects in SIMS are negligible in these experimental conditions. The other important factor considering for the composition analysis of CIGS solar cell by the SIMS depth profile is the deposition inside narrow gap between the CIGS crystal grains during the succeeded process of buffer and window layers. In this case, the result of SIMS depth profile should be deeply related to the packing density of CIGS absorber layer and to the order of deposition. We can be also sure that the wedge depositions into CIGS layer can be negligible in our samples because our grown CIGS absorber layers have relatively high packing density.

3.1 Diffusivity of Zn atoms in the CIGS absorber layer

Figure 3(a) shows the results of the SIMS analysis for a zinc element in both samples A and B. In this figure, the solid circles and the open circles represent the experimental data of sample A and sample B, respectively, while the red and blue solid lines represent the theoretical fit of the respective experimental data with Eq. (1). Generally, the diffusivity of the foreign impurity atoms in CIGS is affected by the intrinsic defect density related to the non-molecularity, $\Delta m = \frac{[Cu]}{[In]} - 1$, and the non-stoichio-metry, $\Delta y = \frac{[2Se]}{([Cu]+[In])} - 1$ in the crystal. Even though, as seen in Fig. 2(c), the variations of Cu, In, Ga and Se counts (c/s) near the junction boundary of CIGS absorbers have somewhat different shapes in each solar cell, all have the same overall shape. Since the SIMS intensities of all the elements near the edge of sample A are somewhat higher than those of sample B, those slight differences may not be due to an actual composition difference but to morphology roughness. In the diffusion process, Zn atoms that diffused from the window or buffer layer to the absorber layer may mainly be substituted for cation atoms such as Cu, or In(Ga) in the CIGS absorber. Filling Zn atoms into Cu vacancies may be the most probable diffusion case in the CIGS solar cell. The results fitted with Eq. (1) are shown in Fig. 3(a). Diffusion coefficients of Zn atom in CIGS, D_{Zn}, at 423K were $2.0 \times 10^{-13} cm^2/s$ and $1.5 \times 10^{-13} cm^2/s$ for sample A and sample B, respectively. Diffusion of Zn into the absorber has been reported for CIGS/CBD-ZnO and CIGS/CBD-Zn(S,O)[5, 6].

The diffusion coefficients of Zn obtained in the present study are in reasonable agreement with those in $CuInSe_2$ bulk crystals in previous experimental data[7]. As seen in Fig. 3(a), there is a small region in the SIMS depth profile which does not fit well with Eq. (1). This suggests that there may be an additional interfacial diffusion process occurring. Previous first-principle calculations support the model of Cu-depletion at the interface between CdS and CIGS[8, 9]. In the case of the $CuInS_2$ absorber and ZnS/Zn(S,O) bilayer buffer, an interdiffusion of Zn and Cu at the interface has been suggested[10]. More extensive studies are needed to elucidate the microscopic mechanism of diffusion in CIGS solar cells.

3.2 Diffusivity of Cd atoms in the CIGS, Zn(S,O) and ZnO

The SIMS experimental data of the Cd atoms and the curve-fit results with Eq. (1) of both sample A(solid circles (meas.), red solid line(fit. CIGS side), and violet dotted line(fit. ZnO side)) and sample B(open circles(meas.) blue solid line(fit. CIGS side), and green dotted line(fit. Zn(S/O) side)) are shown in Fig. 3(b). The diffusion of Cd into the absorber has been observed for CIGS/CBD-CdS by energy dispersive x-ray spectroscopy(EDX)[11, 12] and SIMS[13], which is consistent with the present results.

The diffusion coefficients of the Cd atoms, D_{Cd}, in the CIGS obtained from a curve fit to the experimental data were $4.6 \times 10^{-13} cm^2/s$ for sample A and $4.4 \times 10^{-13} cm^2/s$ for sample B at 423K.

Those values for each sample are within the experimental error. The previous EDX study on $CuInSe_2$ single crystal absorber and CBD-CdS buffer indicates no Cd in the surface of the $CuInSe_2$ [12].

A morphology variation in the ZnO/CdS/SIGS has been reported at high temperatures due to Cd diffusion[14]. No such structure was detected in the present experiment performed at 423K.

A narrow peak located at a depth of 1350 nm was found in sample A. On the other hand, this peak did not exist in sample B. This also agrees well with TEM results. As seen in the TEM spectrum, a CdS layer around 25 nm in thickness was present in sample A, but no distinguishable layer was present in sample B. From SIMS data and TEM spectra, it seems that Cd did not exist as a CdS compound(as buffer) in sample B but existed as Cd

impurity in the CIGS absorber. Even though the diffusion time of sample B was much longer than that of sample A, the diffusion depth of Cd in sample B was smaller than that of sample A, as seen in Fig. 3(b). It seems that this smaller diffusion depth was due to the restricted amount of Cd in sample B. We noted that the diffusivity of Cd was almost two times larger than that of Zn. Moreover, as seen in the left side of Fig. 3(b), the diffusivities of Cd atoms into ZnO:B(sample A) or Zn(S/O)(sample A) layers were extremely low at 423 K. Nevertheless, Cd diffused into the different materials, ZnO:B or Zn(S/O), in each sample, and the estimated diffusion coefficients were almost the same, both being less than $2.2 \times 10^{-15} cm^2/s$. It is believed that Cd did not diffuse back into the window layer during the growth process.

3.3 Diffusivity of S atoms in the CIGS and ZnO

Both SIMS experimental data for S atoms and theoretical fit results are shown in Fig. 3(c). In this figure, solid(sample A) and open circles(sample B) represent the experimental results, while the red and blue solid lines and the violet and green dotted curves represent the respective theoretical fits to the experimental data based on Eq. (1). The diffusion coefficients, D_S, of S atoms in CIGS were $1.6 \times 10^{-13} cm^2/s$ for sample A and $1.8 \times 10^{-13} cm^2/sec$ for sample B at 423K, while the diffusion coefficient of S atoms in ZnO was $3.0 \times 10^{-15} cm^2/s$ for both samples A and B at the same temperature. The starting point of the SIMS signal for S in sample B appeared earlier than that in sample A not only because of the CdS layer, but also because the Zn(S,O) layer in sample B contains S atoms. The estimated thickness of the Zn(S/O) layer in sample B from Fig.3(c) was about 250nm. Moreover, there were signs of accumulation of S atoms at the junction interfaces located at a depth of 1320nm from the top surface of the ZnO window of sample B (in case of sample A, at a 710nm depth), consistent with previous experimental data for CIGS/ALD-Zn(S,O)[15] and $Cu(In,Ga)(S,Se)_2$/CBD-Zn(S,O)[16]. Even though S atoms readily diffuse into CIGS, they do not diffuse back into the ZnO window layer during the growth process. This result agrees wells with a theoretical study of X.F.F an *et al*[8]. According to Fan *et al*.'s theoretical calculation, the Zn-O bond has more ionic characteristics than the Zn-S bond. It is well known that the compounds with stronger polar bonds have a tendency to crystallize in structures with larger Madelung constants. Therefore, ZnS prefers to crystallize in the zincblende (ZB), and ZnO prefers to crystallize in the wurtzite (WZ) structure because the Madelung constant of the WZ structure, 1.641, is greater than that of the ZB structure, 1.638. In addition, the phase transition point from WZ structure to ZB structure in ZnO_xS_{1-x} solid solution alloy was roughly estimated to be x = 0.75. They also calculated the Helmholtz free energy in this solid state system to estimate the equilibrium solubility limits at certain temperatures. They argued that the synthesis of random ZnO and ZnS solid solution at low temperature is almost impossible because the complete miscible critical temperature for this concentration is around 4000 Kelvin for both crystal structures[17].

3.4 Diffusivity of B atoms in the CIGS and Zn(S,O)

Studying the thermal diffusion properties of boron (B) atoms in CIGS is very important because boron-doped ZnO TCO is widely used in CIGS solar cells as a window layer. Boron SIMS data and its theoretical fit results are shown in Fig. 3(d). In this figure, solid(sample A) and open circles(sample B) represent the experimental data, while the colored solid lines represent the theoretical fit to the experimental data.

The diffusion coefficients of B atoms, D_B, were $1.2 \times 10^{-12} cm^2/s$ in CIGS absorber(sample A) and $2.1 \times 10^{-14} cm^2/s$ in Zn(S,O) buffer(sample B) at 423K. As seen in Table 1, the diffusion coefficient of B atoms in CIGS absorber (sample A) was almost one order larger than that of Zn, S, or Cd, while its value in Zn(S,O) film was almost two orders of magnitude smaller than those in the other elements. Moreover, there is also sign of accumulation of B and sulfur atoms at the junction interfaces. The fit results are summarized in Table 1. Experiments employing an ion implantation technique on Ga[18] or In[19] diffusions in ZnO suggest interstitialcy and vacancy-mediated mechanisms. However, the activation energy for In diffusion was reported to be small compared with that in the vacancy mechanism. The experimental diffusion constants of Ga and In in the temperature range around 1123K and 1173K in those references are comparable to the present diffusion constant of B

Table 1. Diffusion coefficients of Zn, Cd, S and B atoms at 423 K.

Element	Diffusion coefficient, D (cm^2/sec), at 423K	
	CIGS/t-CdS/ZnO:B (Sample A)	CIGS/vt-CdS/Zn(S,O)/ZnO:B (Sample B)
Zn	2.0×10^{-13}	1.5×10^{-13}
Cd	4.6×10^{-13}	4.4×10^{-13}
S	1.6×10^{-13}	1.8×10^{-13}
B	1.2×10^{-12}	2.1×10^{-14}

at 423K in CIGS/t-CdS/ZnO:B(sample A). P. Erhar *et al*. claimed that Zn self-diffusion in ZnO occurs via a vacancy mechanism under O-rich and *n*-type conditions based on the GGA+*U* approach[20]. However, A. Janotti *et al*. assumed Zn-rich and *n*-type conditions for their analysis based on the LDA and LDA+*U* approach[21], and G.-Y. Huang *et al*. calculated an activation energy of 2.03 eV, based on the GGA approach, for the vacancy-mediated B diffusion under Zn-rich and *n*-type conditions[22]. On the other hand, a hybrid Hartree-Fock density functional study suggested that Zn vacancies are energetically unfavorable under Zn-rich and *n*-type conditions[23]. G.-Y. Huang *et al*. also pointed out that a fraction of Ga is usually situated in interstices after growth and doping[24]. M. A. N. Nogueira *et al*. reported enhanced Zn self-diffusion in Al-doped ZnO by means of the residual activity method and suggested the incorporation of Al in interstitial sites[25]. H. Ryoken *et al*. found non-equilibrium defects in Al-doped ZnO and suggested the necessity of considering non-equilibrium compensated defects in doped ZnO films prepared at relatively low temperature.[26] In light of those results, the presence of the interstitial B in ZnO is also likely. Since interstitial Ga is calculated to have a small migration barrier[24], the larger diffusion coefficient in CIGS/t-CdS/ZnO:B(sample A) may be attributed to the interstitial B or some non-equilibrium defects. The diffusion coefficient of B in CIGS/vt-CdS/Zn(S,O)/ZnO:B(sample B) is about two orders of magnitude smaller compared with that in CIGS/t-CdS/ZnO:B s(sample A). B diffusion is known to be much slower in Ge than in Si despite the similar crystallographic structure[27]. Furthermore, Ge in SiGe alloys is known to retard transient enhanced diffusion of B[28]. Since the chemical environment around B is very different in ZnO and ZnS, the retardation of B diffusion in the ZnS region seems to be reasonable. Indeed, the defect formation energies for native point defects in ZnS are reportedly very different from those in ZnO[29]. To clarify the B diffusion mechanism in detail, more extensive experimental and theoretical works are needed.

4. Conclusion

Two different window-structured CIGS solar cells, CIGS/t-CdS/ZnO:B(sample A) and CIGS/vt-CdS/ Zn(S,O)/ZnO:B (sample B), were prepared, and the diffusivities of Zn, Cd, S and B atoms in CIGS, ZnO and Zn(S,O) were estimated by a theoretical fit to the experimental SIMS data. Diffusion coefficients of Zn atoms, D_{Zn}, in CIGS were $2.0 \times 10^{-13} cm^2/s$ and $1.5 \times 10^{-13} cm^2/s$ for sample A and for sample B, respectively, at 423K. The diffusion coefficients of Cd atoms, D_{Cd}, in CIGS were $4.6 \times 10^{-13} cm^2/s$ for a sample A and $4.4 \times 10^{-13} cm^2/s$ for a sample B at 423K. The diffusivity of Cd in CIGS was almost two times larger than that of Zn. Moreover, the diffusivities of Cd atoms diffusing back into ZnO(sample A) or Zn(S,O) (sample A) layers were extremely low at 423K, and the estimate diffusion coefficients were both close to $2.2 \times 10^{-15} cm^2/s$.

The diffusion coefficients of S atoms, D_S, in CIGS were $1.6 \times 10^{-13} cm^2/s$ for a sample A and $1.8 \times 10^{-13} cm^2/s$ for a sample B at 423K, while the diffusion coefficient of S in ZnO was $3.0 \times 10^{-15} cm^2/s$ for both samples. The diffusion coefficients of B atoms, D_B, were $1.2 \times 10^{-12} cm^2/s$ in CIGS absorber (sample A) and $2.1 \times 10^{-14} cm^2/s$ in Zn(S,O) buffer (sample B) at 423K.

Acknowledgement

This work of I. H. Choi was supported by a Center for Inorganic Photovoltaic Materials(No. 2012-0001168) grant funded by the Korean government(MEST). The work of Y. G. Yoon was supported by the Basic Science Research Program through the National Research Foundation of Korea(NRF) funded by the Ministry of Education, Science and Technology under contract No. 2011-0002919.

References

1. I. Repins, M. A. Contreras, B. Egaas, C. DeHart, J. Scharf, C. L. Perkins, B. To, and R. Noufi, “19.9% - efficient ZnO/CdS/CuInGaSe$_2$ solar cell with 81.2% fill factor”, Prog. Photovoltaics Prog. 16, pp. 235, 2008.
2. D. Hariskos, S. Spiering, and M. Powalla, “Buffer layers in Cu(In,Ga)Se$_2$ solar cells and modules”, Thin Solid Films, Vol. 480–481, pp. 99-109, 2005.
3. S. Siebentritt, “Alternative buffers for chalcopyrite solar cells”, Sol. Energy Vol. 77, pp. 767, 2004.
4. O. Cojocaru-Mirédin, P. Choi, R. Wuerz, and D. Raabe, “Atomic - scale characteriza -tion of the CdS/CuInSe$_2$ interface in thin-film solar cells”, Appl. Phys. Lett., 98, pp. 103504, 2011.
5. T. Nakada, T. Kume, T. Mise, and A. Kunioka, “Superstrate-Type Cu(In,Ga)Se$_2$ Thin Film Solar Cells with ZnO Buffer Layers”, Jpn. J. Appl. Phys., Vol.37, L499 1998.
6. T. Nakada, M. Hongo, and E. Hayashi, “Band offset of high efficiency CBD-ZnS/CIGS thin film solar cells”, Thin Solid Films, 242, pp. 431-432, 2003.

7. M. Benabdeslem, N. Benslim, L. Bechiri, L. Mahdjoubi, E. B. Hannech, and G. Nouet, "Diffusion of Zn in $CuInSe_2$ bulk crystals", J. Cryst. Growth., Vol, 274, pp. 144-148, 2005.
8. J. Pohl, A. Klein, and K. Albe, "Role of copper interstitials in $CuInSe_2$: First - principles calculations", Phys. Rev. B, Vol. 84, 121201(R), 2011.
9. R. Herberholz, U. Rau, H. W. Schock, T. Haalboom, T. Gödecke, F. Ernst, C. Beilharz, K. W. Benz, and D. Cahen, "Phase segregation, Cu migration and junction formation in Cu(In, Ga)Se_2", Eur. Phys. J.-Appl. Phys 6, 131 (1999).
10. M. Bär, A. Ennaoui, J. Klaer, T. Kropp, R. Sáez-Araoz, S. Lehmann, A. Grimm, I. Lauermann, Ch. Loreck, St. Sokoll, H.-W. Schock, Ch.-H. Fischer, and M. C. Lux-Steiner, and Ch. Jung, "Intermixing at the heterointerface between ZnS/Zn (S,O) bilayer buffer and CuInS2 thin film solar cell absorber", J. Appl. Phys., Vol. 100, 064911, 2006.
11. T. Nakada and A. Kunioka, "Direct evidence of Cd diffusion into Cu(In, Ga)Se_2 thin films during chemical-bath deposition process of CdS films", Appl. Phys. Lett., Vol. 74, pp. 2444, 1999.
12. T. Nakada, "Nano - structural investiga -tions on Cd-doping into Cu(In,Ga)Se_2 thin films by chemical bath deposition process", Thin Solid Films, Vol. 361-362, pp. 346-352, 2000.
13. S. Kijima and T. Nakada, "High - Temperature Degradation Mechanism of Cu(In,Ga)Se_2-Based Thin Film Solar Cells", Appl. Phys. Express 1, 075002, 2008.
14. S.-Y. Park, E.-W. Lee, S.-H. Lee, S.-W. Park, W.-K. Kim, S.-H. Lee, W.-G. Lee, B.-J. Lee, H.-K. Bae, J.-H. Yoo, and C.-W. Jeon, "Investigation of ZnO/CdS/$CuIn_xGa_{1-x}Se_2$ interface reaction by using hot-stage TEM", Curr. Appl. Phys. 10, S399, 2010.
15. C. Platzer-Björkman, T. Törndahl, D. Abou-Ras, J. Malmström, J. Kessler, and L. Stolt, "Zn(O,S) buffer layers by atomic layer deposition in Cu(In,Ga)Se_2 based thin film solar cells: Band alignment and sulfur gradient", J. Appl. Phys. 100, 044506, 2006.
16. R. Sáez-Araoz, D. Abou-Ras, T. P. Niesen, A. Neisser, K. Wilchelmi, M. Ch. Lux-Steiner, and A. Ennaoui, "In situ monitoring the growth of thin-film ZnS/Zn(S,O) bilayer on Cu-chalcopyrite for high performance thin film solar cells", Thin Solid Films, Vol. 517, pp.2300, 2009.
17. X. F. Fan, Z. X. Shen, Y. M. Lu, and J. L. Kuo, "A theoretical study of thermal stability and electronic properties of wurtzite and zincblende ZnOxS1−x", New J. phys., 11, 093008, 2009.
18. T. Nakagawa, I. Sakaguchi, M. Uematsu, Y. Sato, N. Ohashi, H. Haneda, and Y. Ikuhara, "Diffusion Model of Gallium in Single-Crystal ZnO Proposed from Analysis of Concentration-Dependent Profiles Based on the Fermi-Level Effect", Jpn. J. Appl. Phys. 46, 4099, 2007.
19. T. Nakagawa, K. Matsumoto, I. Sakaguchi, M. Uematsu, H. Haneda, and N. Ohashi, "Analysis of Indium Diffusion Profiles Based on the Fermi-Level Effect in Single-Crystal Zinc Oxide", Jpn. J. Appl. Phys. 47, 7848, 2008.
20. P. Erhart and K. Albe, "Diffusion of zinc vacancies and interstitials in zinc oxide", Appl. Phys. Lett. 88, 201918, 2006.
21. A. Janotti and C. G. Van de Walle, "Native point defects in ZnO", Phys. Rev. B 76, 165202, 2007.
22. G.-Y. Huang, C.-Y. Wang, and J.-T. Wang, "Vacancy-assisted diffusion mechanism of group-III elements in ZnO: An ab initio study", J. Appl. Phys., 105, 073504, 2009.
23. F. Oba, A. Togo, I. Tanaka, J. Paier, and G. Kresse, "Defect energetics in ZnO: A hybrid Hartree-Fock density functional study", Phys. Rev. B, 77, 245202, 2009.
24. G.-Y. Huang, C.-Y. Wang, and J.-T. Wang, "First-principles study of the diffusion of Ga via interstitial-mediated mechanisms in ZnO", Scr. Mater., 61, 324, 2009.
25. M. A. N. Nogueira, A. C. S. Sabioni, and W. B. Ferraz, "Zinc Self-Diffusion in ZnO", Defect and Diffusion Forum, 237-240, 163, 2005.
26. H. Ryoken, I. Sakaguchi, N. Ohashi, T. Sekiguchi, S. Hishita, and H. Haneda, "Non - equilibrium defects in aluminum - doped zinc oxide thin films grown with a pulsed laser deposition method", J. Mater. Res., 20, 2866, 2005.
27. E. Bruno, S. Mirabella, G. Scapellato, G. Impellizzeri, A. Terrasi, F. Priolo, E. Napolitani, D. De Salvador, M. Mastromatteo, and A. Carnera, "Mechanism of B diffusion in crystalline Ge under proton irradiation", Phys. Rev. B, 80, 033204, 2009.
28. L. Wang, P. Clancy, and C. S. Murthy, "First-principles study of the origin of retarded diffusion of boron in silicon in the presence of germanium", Phys. Rev. B, 70, 165206, 2004.
29. Y. Gai, J. Li, B. Yao, and J.-B. Xia, "The bipolar doping of ZnS via native defects and external dopants", J. Appl. Phys., 105, 113704, 2009.